

MULTIDIMENSIONAL TURBULENCE SPECTRA - STATISTICAL ANALYSIS OF TURBULENT VORTICES

Farideh GHASEMPOUR*, Ronnie ANDERSSON and Bengt ANDERSSON

Department of Chemical and Biological Engineering, Chalmers University of
Technology, SE-41296 Gothenburg, Sweden

*Corresponding author, E-mail address: farideh@chalmers.se

ABSTRACT

Strong nonlinear or very fast phenomena, e.g. mixing, coalescence and breakup, are not correctly described using average turbulence properties. The main mechanism behind these fast phenomena is an interaction with single or paired vortices and therefore, the properties of individual turbulent vortices should be investigated and understood. For this reason statistical analysis of turbulent vortices was performed using the developed vortex tracking algorithm. Turbulence was modeled using large eddy simulations with the dynamic Smagorinsky-Lilly subgrid scale model for two different Reynolds numbers. The number density of turbulent vortices and their properties including enstrophy and core size identified by the Q-criterion were described as a function of spatial positions. The number density computed by the developed vortex tracking algorithm was highly compatible with the models suggested by Batchelor and Martinez in the inertial subrange and reasonable agreement was found for larger vortex sizes. Moreover, it was concluded that the associated enstrophy within the same size of coherent structures found by the Q criterion had the same wide distribution function as turbulent kinetic energy.

NOMENCLATURE

E	turbulent energy spectrum
L_0	largest turbulent vortices length scale
\dot{n}	number density
\vec{u}_λ	fluctuating velocity of turbulent vortices of sizes λ
ε	turbulent energy dissipation rate
η	Kolmogorov scale
λ	vortex sizes and Taylor micro scale
κ	wave number
ρ	density
Re_λ	Taylor scale Reynolds number
α	constant in the Eq. 3
β	constant in the Eq. 2
$\bar{e}(\lambda)$	average vortex energy for a vortex size λ

INTRODUCTION

Most flows in chemical engineering processes are turbulent and often they consist of two or more phases. Simulation of these systems is complex and requires a detailed description of the turbulence spectra (Deshpande et al., 2010). Detailed description of turbulence is needed to model and quantify their behavior. Phenomena such as

coalescence and breakage occur very fast, often within a few milliseconds (Andersson and Andersson, 2006b). This time scale is equal to or smaller than the life time of the turbulent vortices for many engineering applications (Andersson et al., 2004) and thus, there is no time to interact with the statistical mean of turbulent kinetic energy and the interaction is better described by the properties of single turbulent vortices.

Consequently, it is not sufficient to know only the average turbulence properties to model these phenomena (Andersson and Andersson, 2006a, Andersson et al., 2004, Luo and Svendsen, 1996). Therefore, data on vortex size, lifetime, number density (the number of turbulent vortices per unit fluid volume), growth and dissipation rate, and the distribution of turbulent kinetic energy for vortices of different sizes at different locations are needed. With reference to aforementioned turbulence parameters, a notable one is the vortex number density. The distribution of strong vortices, their number density and size are a part of "wish list" for current and future studies in order to understand the fundamentals of turbulence (Marseille, 2011). Volume and number density of vortices in a fully turbulent flow are a part of the most important key parameters for the study of coalescence and breakage processes.

A practical reason for studying the volume and number density of vortices is that models at hand for breakup and coalescence are valid for specific cases. No model is available which is valid for a wide range of flow situations (Liao and Lucas, 2009, Liao and Lucas, 2010). Moreover the eddy number distributions can be used to derive expressions relating to the fractional rate of surface renewal and mass transfer coefficients across gas-liquid and solid-liquid interfaces (Zhang and Thomas, 1996). For these reasons a systematic evaluation of available models on number density is required as a foundation for further investigations.

In this paper statistical analysis of turbulent vortices was performed using the developed vortex tracking algorithm. The number density of turbulent vortices and their properties including enstrophy and core size found by the Q-criterion were described as function of size and radial position at two different flow conditions.

MODELING OF VORTEX NUMBER DENSITY

Generally, the number density of turbulent vortices, \dot{n} , is defined as the number of turbulent vortices per unit fluid volume. A relationship between the number density of turbulent vortices of sizes between λ and $\lambda + d\lambda$ and the

turbulent energy spectrum, $E(\kappa)$, can be formulated by writing an energy balance for vortices of wave number between κ and $\kappa+d\kappa$ in the inertial subrange

$$\dot{n}_\lambda \rho_c \frac{\pi}{6} \lambda^3 \frac{u_\lambda^2}{2} d\lambda = E(\kappa) \rho_c (-d\kappa) \quad (1)$$

Here, the wave number, κ , is $2\pi/\lambda$. \bar{u}_λ is the mean fluctuating velocity of turbulent vortices of size λ and it is given by,

$$\bar{u}_\lambda = \beta^{1/2} (\varepsilon \lambda)^{1/3} \quad (2)$$

The energy spectrum in the inertial subrange is

$$E(\kappa) = \alpha \varepsilon^{2/3} \kappa^{-5/3} \quad (3)$$

On substituting of Eqs. 2 and 3 into Eq. 1 the number density of turbulent vortices of sizes between λ and $\lambda+d\lambda$ is given by

$$\dot{n}_\lambda = \frac{C_1}{\lambda^4} \quad (4)$$

$$C_1 = \frac{24\alpha}{(2\pi)^{5/3} \beta} \quad (5)$$

Different values for the coefficient C_1 in the literature are summarized in Table 1. The experimental data shows that the constant α is 1.5 approximately (Lumley, 1972). A number of authors report very different estimates for β as they are shown in Table 1.

Table 1. Various coefficients in the number density models in the literature.

Model	β	C_1
Jakobsen (Jakobsen, 2008)	2	0.841
Luo & Svendsen (Luo and Svendsen, 1996)	$\beta=8C_2/(3*\pi)$, $C_2=2.41$	0.822
Batchelor (Batchelor, 1982)	7.23	0.2327
Pope (Pope, 2000)	1.973	0.8528
Martinez (Martinez-Bazan et al., 1999)	8.2	0.2052

Several number density models for turbulent vortices suggested in the literature were applied and compared with the number density of turbulent vortices identified with the vortex tracking algorithm. Risso and Fabre (Risso and Fabre, 1998) have used the same value as given by Pope (Pope, 2000) and Lasheras (Lasheras et al., 2002) has pointed out that there is a range for β between 2.045 and 8.2. Therefore, his results would vary between the Jakobsen and Martinez models.

Computational details

In this work, turbulence was modeled using large eddy simulations (LES) with the dynamic Smagorinsky-Lilly subgrid scale model. The simulations were performed for a turbulent pipe flow ($\varnothing=5$ cm, $L=20$ cm) of water at two different Reynolds numbers, 20000 and 50000 respectively. Using periodic boundary conditions, more than 97% of the total turbulent kinetic energy in the bulk of the flow and more than 80% at $y^+ > 5$ is captured. Below $y^+=5$ the subgrid turbulent viscosity ratio is lower than 0.1 and the maximum subgrid turbulent viscosity ratio in the bulk of the flow is 1.55. The maximum instantaneous and average wall y^+ are 1.7 and 0.85 respectively, which are in the accepted region for LES simulation (Pope, 2004).

Eddy identification and analysis methods

Several Eulerian methods for identifying flow structures are proposed in the literature. They are generally formulated in terms of the invariants of the velocity gradient tensor. These criteria are the iso-surfaces of vorticity, Q criterion, complex eigenvalues of the velocity gradient tensor, λ_2 and pressure minimum. Chakraborty and et al. showed that the Q criterion and λ_2 almost give the same flow structures (Chakraborty et al., 2005).

When there is no imposed non-uniform strain field in the turbulent flow, the Q-criterion can be used to identify the core location of the turbulent vortices. The Q-criterion represents the local balance between rotation and strain rate. To identify a wide range of vortices even the weakest one in the bulk, the Q-criterion can be normalized with respect to the rotation rate (Ghasempour et al., 2011).

In this research work a 3D image segmentation algorithm was developed to identify individual vortices. By using the algorithm, the cores of the coherent structures identified by Q criterion were found. Previously, an analysis of the turbulent energy outside the iso-surface of Q criterion revealed that less than 40% of the turbulent kinetic energy (TKE) would be within the structures identified by Q criterion (Ghasempour et al., 2011). This occurs because the Q criterion represents just the vortex cores even with the lowest possible cut off criterion. As pointed out in the literature, turbulent kinetic energy is one of the key parameters in the breakage, coalescence and mixing phenomena. Thus, capturing almost 85% of the turbulent kinetic energy by coherent structures was aimed.

Since the iso-Q surface is located very close to the peak in turbulent kinetic energy (Figure 1), extending the calculated volumes by Q criterion would compensate the lack of aimed TKE. Figure 1 shows the distribution of turbulent kinetic energy for an idealized Lamb-Oseen vortex. Unfortunately it is not possible to determine how much the volume should be extended from this data, since the idealized vortex is not affected by neighboring vortices and the energy dissipation in the fluid. Consequently the extension would be overestimated.

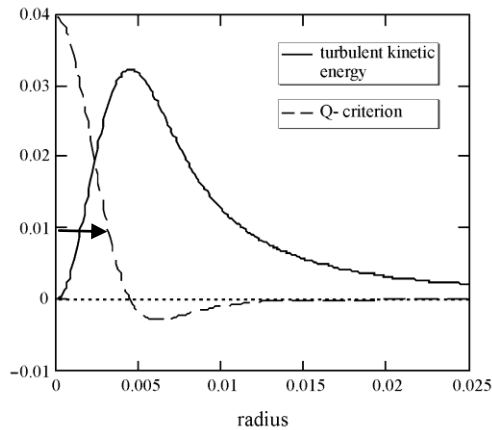


Figure 1. The Q-criterion and the turbulent kinetic energy in an idealized Lamb-Oseen vortex. The arrow indicate the vortex size estimated with normalized $Q > 0.2$.

Instead the extension criterion was obtained by analyzing the LES data. In a pipe cross-section plane, shown in Figure 2, the ratio of the surface of coherent structures associated with 85% TKE to the identified surface connected by the Q-criterion was around 2.54. The axial length of the turbulent structures was captured accurately with the Q-criterion while the radial size was underestimated, therefore all volumes identified by the vortex tracking algorithm were multiplied by 2.5 to get closer to the aimed conditions.

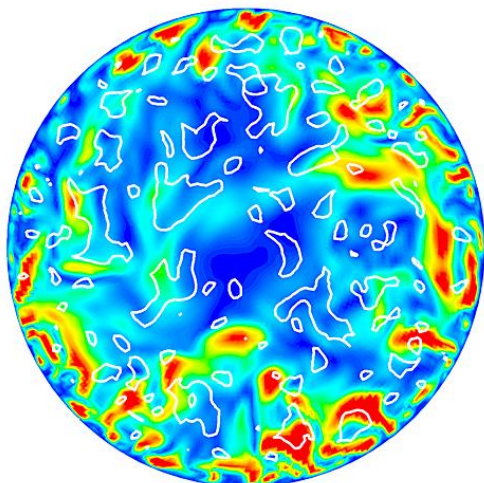


Figure 2. Overlap of turbulent kinetic energy and turbulent structures identified by normalized iso-Q criterion. The colour shows the TKE and the white iso-lines show the Q criterion.

According to Figure 2, the turbulence parameters are varying with the pipe radius and most of them are generated in areas with high shear rate. Hence, it was highly motivated to do statistical analysis at different radial locations. Therefore, the analysis was done for 5 equally spaced radial fractions.

By using the vortex volumes found by the Q-criterion, the diameter of equivalent spheres was calculated in order to make a comparison with data in the literature possible e.g. (Luo and Svendsen, 1996). Data sampling and statistical analysis were performed at three different pipe segments. Three six-centimeter axial pipe segments:

'Initial', 'Middle' and 'End' parts were considered. This helps to assess the stability of the analyzed data.

RESULTS AND DISCUSSION

In this study, the turbulence properties: number density, enstrophy, vortices core size and vortex location were computed from LES simulation of a turbulent pipe, by using the vortex tracking algorithm. The analysis was carried out for two different Reynolds number, 20000 and 50000. As shown in Table 2, more than 8100 and 13300 vortex cores were identified at these two flow conditions respectively.

Table 2. Turbulence properties.

	Re=20000	Re=50000
Re_λ	80	101
Number of vortices identified	8147	13355

Further, the distribution of number density at different radial segments of pipe was analyzed.

Number density models for turbulent vortices

The number density of turbulent vortices was calculated using relevant literature models, Table 1, and compared with the results obtained with the vortex tracking algorithm developed in this project. In fact, the number density of turbulent vortices of various models was calculated for vortex sizes between λ and $\lambda + d\lambda$. In this work, the bin sizes were small for the smaller vortices and their sizes were increasing gradually for the larger ones. By considering the real volume for coherent structures the identified volumes for each bin was moved to the corresponding real bin using the extended volume discussed in the previous section. The factor 2.5 discussed in the previous section is a global value. Work is in progress using Biot-Savart analysis to further investigate the validity of this value (Ghasempour, et al.)

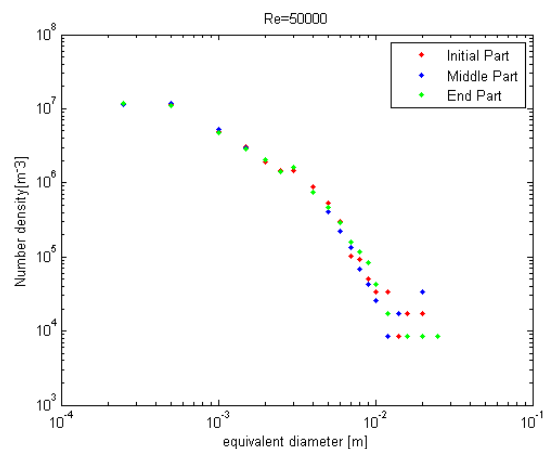


Figure 2. Number density of turbulent vortices identified with the vortex tracking algorithm, at different spatial locations.

In Figure 3, the number density of turbulent vortices at three different pipe segments is compared. As seen in Figure 3, the number densities in these segments (Initial, Middle and End) have the same distribution for smaller vortices. But for the larger vortices the number densities deviate, mainly due to the low number of large vortices.

In Figure 3, one can see that the quantified number density, by means of the vortex tracking algorithm, has similar form as the modeled ones. Particular the number densities computed with the Batchelor and Martinez models agrees very well for vortex sizes between 2.5 mm and 18 mm. For the other models, the minimum ratio of modeled number density to the quantified number density was around 3 at large equivalent diameters.

All these models are valid in the inertial subrange, and in this case a lower range of the inertial subrange is expected at 1-5 mm depending on the model used for estimation. For smaller vortices there is a significant deviation. Below the inertial subrange all the models over predict the number density. This is expected since dissipation of turbulent kinetic energy occurs at small turbulent scales.

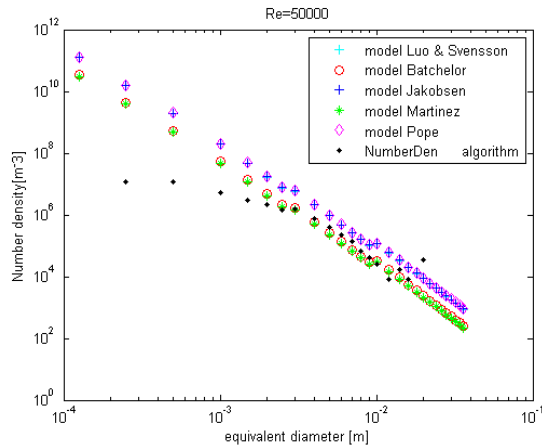


Figure 3. Comparison between number density identified with the vortex tracking algorithm and the different models.

The number density of turbulent vortices is shown as a function of the radial position in Figure 4. As shown here the number density of turbulent vortices calculated with the Batchelor and Martinez models, agrees somewhat better nearby the pipe wall ($0.8 < r/R < 1$) than in the core of the pipe.

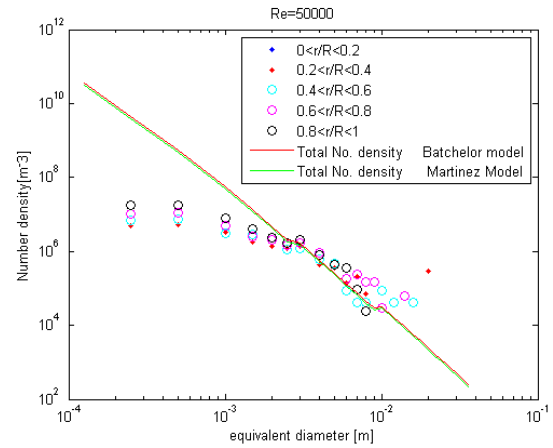


Figure 4. Number density of turbulent vortices at different radial locations.

Theoretically, by increasing the Reynolds number, the inertial subrange in a turbulent flow is increased (Andersson, et al. 2012). At the same time the number density of the turbulent vortices from various models are valid only for inertial subrange. As shown in Figure 5, the range over which the number densities are following the modelled line, is larger in the case of higher Reynolds number i.e. at $Re=50000$, which is expected.

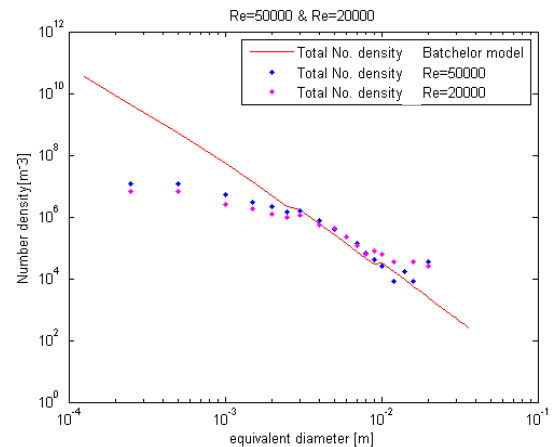


Figure 5. Number density of turbulent vortices at different Reynolds numbers.

Vorticity and core size found by the Q-criterion

Moreover, the vortex tracking algorithm also reveals details of the vortex statistical properties including enstrophy distribution. An analysis of the associated enstrophy within turbulence coherent structures found by the Q-criterion shows that the volume weighted enstrophy is increasing with the equivalent diameters of the vortices. The volume weighted enstrophy is shown as a function of the five radial locations in Figure 6. The number of vortices is clearly increasing in a direction from core to the wall pipe, and the amount of volume weighted enstrophy linked by vortices is increasing in the near wall region.

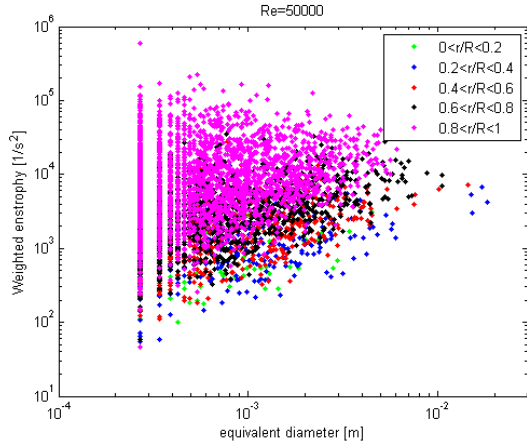


Figure 6. Volume weighted enstrophy of turbulent vortices at different radial locations.

It is frequently assumed that for each vortex size, λ , there is a distribution of fluctuating velocities and the turbulent kinetic energy probability distribution, $p_e(\phi)$, is given by Angelidou et al. (Angelidou et al., 1979) and Luo and Svendsen (Luo and Svendsen, 1996),

$$p_e(\phi) = \frac{1}{e(\lambda)} \exp(\phi) \quad (6)$$

where

$$\phi = \frac{e(\lambda)}{\bar{e}(\lambda)} \quad (7)$$

Here $\bar{e}(\lambda)$ is the average vortex energy in the inertial subrange for a vortex size λ .

Analogous to the distribution of turbulent kinetic energy, the volume weighted enstrophy distribution of vortices was studied for various vortex sizes. We expect that turbulent kinetic energy should scale with vorticity assuming the fluctuating velocity at the surface of the iso-Q volume can be estimated by $u' \propto \omega R$ and consequently the kinetic energy $k \propto \omega^2 R^2$. The enstrophy should then be distributed according to Eq. (6) in the inertial subrange.

As seen in Figure 7, there is a distribution of connected enstrophy within same size of coherent structures identified by the Q criterion. In this figure it can also be seen that vortices with sizes between 2.6mm and 4.3mm have approximately similar probability distributions and for the vortex sizes smaller than 2.6mm and larger than 4.3mm there are significantly different slopes. In this analysis, the normalized probability distribution of weighted enstrophy for a certain vortex size was normalized based on the trapezoidal integrated surface area beneath the corresponded probability distribution. The lower range of enstrophy is removed since the model is not valid in that range. Also our criterion for selecting vortices, i.e. the normalized Q-criterion, will not identify vortices with low vorticity.

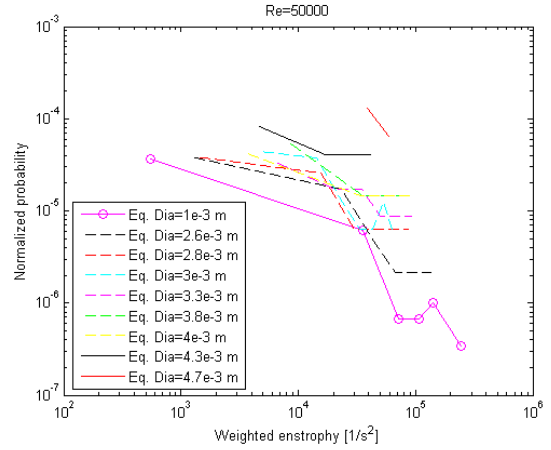


Figure 7. The normalized probability distribution of weighted enstrophy for different vortex sizes.

CONCLUSIONS

The simulations were done at rather low Reynolds numbers 20000 and 50000, corresponding to Taylor scale Reynolds numbers 80 and 101 respectively. At these low Reynolds numbers the inertial subrange is very narrow. However, these flow conditions are close to what is observed in chemical process equipments and motivates a detailed study.

The LES simulations were done with very good resolution. More than 97% of the total turbulent kinetic energy was resolved and the maximum subgrid turbulent viscosity to molecular viscosity ratio was 1.55.

An efficient vortex tracking algorithm that allows identification of thousands of vortices, and quantification of turbulent properties, needed for statistical analysis of turbulence was successfully developed. A separate analysis of the coherent vortices in three different parts of the pipe gave almost identical results, only a random effect was noticed for the largest eddies due to the very low numbers.

The calculated number densities agreed very well in the inertial subrange with the proposed models in the literature. There is some difference in radial position for the larger vortices but no valid conclusions can be drawn since there are too few vortices in each bin size. The effect of Reynolds number is minor with a tendency to a lower slope at lower Reynolds number, but the effect is probably due to a more narrow inertial subrange at lower Reynolds number.

The enstrophy variation for a given vortex size is very large and this variation must be taken into account when estimating properties of turbulent flow e.g. for calculation of break up rate of bubbles and drops.

REFERENCES

- ANDERSSON, R. and ANDERSSON, B. (2006a). "Modeling the breakup of fluid particles in turbulent flows". *AIChE Journal*, **52**, 2031-2038.
- ANDERSSON, R. and ANDERSSON, B. (2006b). "On the breakup of fluid particles in turbulent flows". *AIChE Journal*, **52**, 2020-2030.

- ANDERSSON, R., ANDERSSON, B., CHOPARD, F. and NOREN, T. (2004). "Development of a multi-scale simulation method for design of novel multiphase reactors". *Chemical Engineering Science*, **59**, 4911-4917.
- ANDERSSON, B. ANDERSSON, R. HÅKANSSON, L. MORTENSEN, M. et al. 2012. *Computational fluid dynamics for engineers*, Cambridge, Cambridge University Press.
- ANGELIDOU, C., PSIMOPOULOS, M. and JAMESON, G. J. (1979). "Size distribution functions of dispersions". *Chemical Engineering Science*, **34**, 671-676.
- BATCHELOR, G. K. 1982. *The theory of homogeneous turbulence*, Cambridge, Cambridge University Press.
- CHAKRABORTY, P., BALACHANDAR, S. & ADRIAN, R. J. (2005). "On the relationships between local vortex identification schemes". *Journal of Fluid Mechanics*, **535**, 189-214.
- DESHPANDE, S. S., TABIB, M. V., JOSHI, J. B., KUMAR, V. R. and KULKARNI, B. D. (2010). "Analysis of flow structures and energy spectra in chemical process equipment". *Journal of Turbulence*, **11**, 1-39.
- GHASEMPOUR, F., ANDERSSON, R., KEVLAHAN, N. and ANDERSSON, B. (2011). "Multidimensional turbulence spectra – identifying properties of turbulent structures". *Journal of Physics: Conference Series*, **318**, 042022.
- GHASEMPOUR, F., ANDERSSON, R., KEVLAHAN, N. and ANDERSSON, B. "Turbulent kinetic energy of coherent vortex structures using the Biot-Savart law". *In manuscript*.
- JAKOBSEN, H. A. 2008. *Chemical reactor modeling - multiphase reactive flows*, Berlin, Springer.
- LASHERAS, J. C., EASTWOOD, C., MARTINEZ-BAZAN, C. and MONTANES, J. L. (2002). "A review of statistical models for the break-up of an immiscible fluid immersed into a fully developed turbulent flow". *International Journal of Multiphase Flow*, **28**, 247-278.
- LIAO, Y. X. and LUCAS, D. (2009). "A literature review of theoretical models for drop and bubble breakup in turbulent dispersions". *Chemical Engineering Science*, **64**, 3389-3406.
- LIAO, Y. X. and LUCAS, D. (2010). "A literature review on mechanisms and models for the coalescence process of fluid particles". *Chemical Engineering Science*, **65**, 2851-2864.
- LUO, H. and SVENDSEN, H. F. (1996). "Theoretical model for drop and bubble breakup in turbulent dispersions". *AIChE Journal*, **42**, 1225-1233.
- JEONG, J. & HUSSAIN, F. (1995). "On the identification of a vortex", *Journal of Fluid Mechanics*, **285**, 69-94.
- MARSEILLE. 2011. *Turbulence Colloquium Marseille 2011* [Online]. Available: <http://www.turbulence.ens.fr>.
- MARTINEZ-BAZAN, C., MONTANES, J. L. and LASHERAS, J. C. (1999). "On the breakup of an air bubble injected into a fully developed turbulent flow. Part 2 size pdf of the resulting daughter bubbles.". *Journal of Fluid Mechanics*, **401**, 183-207.
- POPE, S. B. 2000. *Turbulent flows*, Cambridge, Cambridge University Press.
- POPE, S. B. (2004), "Ten questions concerning the large-eddy simulation of turbulent flows", *New Journal of Physics*, **6**, 35.
- RISSE, F. and FABRE, J. (1998). "Oscillations and breakup of a bubble immersed in a turbulent field". *Journal of Fluid Mechanics*, **372**, 323-355.
- ZHANG, Z. B. and THOMAS, C. R. (1996). "Eddy number distribution in isotropic turbulence and its application for estimating mass transfer coefficients". *Chemical Engineering Communications*, **140**, 207-217.